AD-A090 444 OFFICE OF THE PROJECT MANAGER STANDOFF TARGET ACQUISI--ETC F/G 9/4
NOISE PERFORMANCE OF A NEW TYPE OF LOW NOISE FM DETECTOR,(U)
JUN 80 A B TARBELL

UNCLASSIFIED NL

END
DATE FILMED
11-80
DTIC

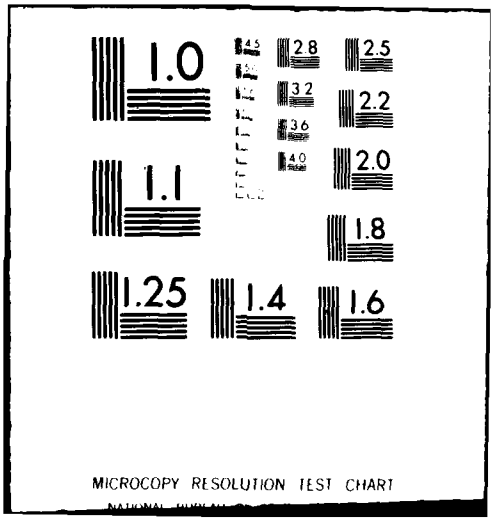
1.0
1.1
1.25
1.4
1.6
1.8
2.0
2.2
2.5
2.8
3.2
3.6
4.0
MICROCOPY RESOLUTION TEST CHART

TARBELL



(12) 15

(6)

# NOISE PERFORMANCE OF A NEW TYPE OF LOW NOISE FM DETECTOR

(10)
DR. ALLAN B. TARBELL
OFFICE OF THE PROJECT MANAGER, SOTAS
FORT MONMOUTH, N. J. 07703

(11) JUN 1980

The development of the wideband quasi-coherent detector described in this paper resulted from the need for a low noise, very low delay FM detector for use in power line protection systems. At NTC-1975, Klapper and Kratt described the new detector and presented the results of their analyses of output distortion and performance in the presence of sine wave interference. Recently they have published a more detailed analysis (1). These previous authors showed that under usual operating conditions the detector output contains distortion components that are relatively small. They also found that in the presence of weak sine wave interference their detector performed approximately the same as the limiter discriminator. However, with a strong interfering carrier the Klapper-Kratt detector performed much better than did the limiter discriminator. The detector's performance in the presence of strong interference led to the inquiry whether the new detector might possibly provide threshold extension.

The detector (without limiter) has now been analyzed with noise and found to perform identically to the limiter discriminator above threshold. However, threshold occurs at a higher CNR than that of the conventional limiter discriminator. The results of this analysis were confirmed experimentally by assembling and testing a version of the new detector family. It was also verified experimentally that the Klapper-Kratt detector preceded by a limiter performs identically to the limiter discriminator.

## Noise Analysis

There are several forms of the Klapper-Kratt detector. In





(325)

this paper, the version shown in Figure 1 was chosen to be analyzed in detail. The primary reason for this choice was determined by the lack of an integrator in the demodulator portion of the detector. With no integrators, the potential integrator initial condition problem previously described[1] is nonexistent resulting in a detector with true wideband performance.

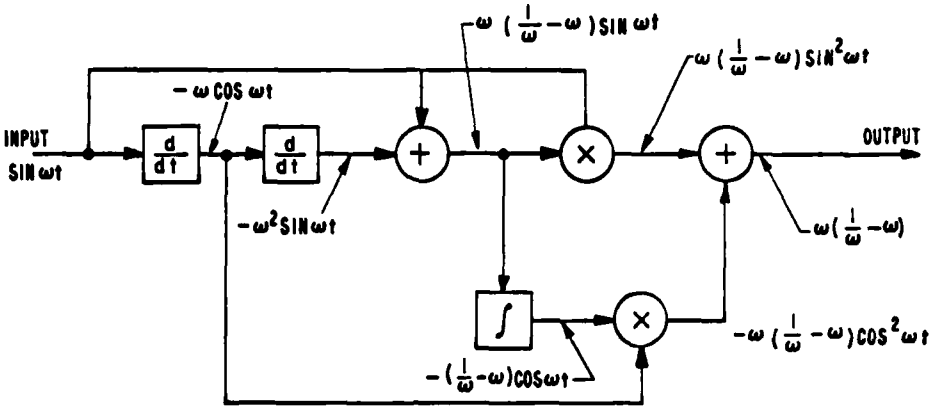


Figure 1. Dual Differentiator Version of The New FM Detector

The operation of the detector may be understood as follows. The input signal is applied to the first differentiator input. The output of the second differentiator is 180° out of phase with the input signal, and the amplitude varies as the square of the instantaneous input frequency. The time constant of each differentiator is selected to give unity gain at some radian frequency, $\omega_c$ . Thus, at this center frequency, the output of the summer vanishes. Above and below this frequency, the output of the summer has an amplitude which increases as the frequency of the input signal moves away from $\omega_c$ . Coherent detection is performed by the first multiplier. The output of this multiplier is a signal containing the demodulated output plus a component at the second harmonic of the detector input signal.

The RF canceller portion of the detector has been added to remove the second harmonic of the input signal with theoretically zero delay. The canceller circuit generates a term proportional to $\sin^2 \omega_c t$ which, when added to the first multiplier output, cancels the second harmonic present in the demodulator output.

A brief description of the derivation of the SNR-CNR relationship will now be presented. The demodulator portion of the detector is redrawn in Figure 2.

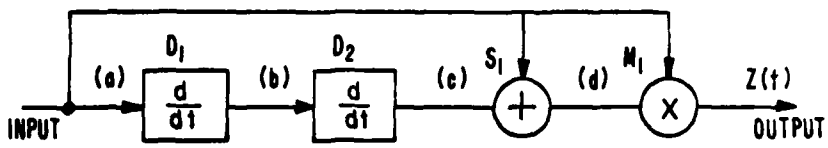


Figure 2. Demodulator Portion of FM Detector

The input signal is assumed to consist of a carrier plus additive narrowband Gaussian noise, or

$$\text{INPUT} = A \sin \omega_c t + \underbrace{x(t) \cos \omega_c t - y(t) \sin \omega_c t}_{\text{NOISE}} \quad (1)$$

where $\omega_c$ is the center frequency.

Passing this signal through the demodulator and completing the indicated mathematical operations results in

$$z(t) = -\frac{A\dot{x}(t)}{\omega_0} - \frac{A\ddot{y}(t)}{2\omega_0^2} + \frac{y(t)\dot{x}(t)}{\omega_c} + \frac{y(t)\ddot{y}(t)}{2\omega_0^2} + \frac{x(t)\ddot{x}(t)}{2\omega_c^2} - \frac{x(t)\dot{y}(t)}{\omega_c} \quad (2)$$

Assuming that $\omega_c^2 \gg \omega_0$, Equation 2 reduces to Equation 3,

$$z(t) = -\frac{A\dot{x}(t)}{\omega_c} + \frac{y(t)\dot{x}(t)}{\omega_0} - \frac{x(t)\dot{y}(t)}{\omega_0} \quad (3)$$



(327)

Next, the autocorrelation of z(t), defined by Equation 4, is determined.

$$R_{zz}(\tau) \equiv E\{z(t)\,z(t+\tau)\} \tag{4}$$

$$R_{zz}(\tau) = E\left\{\left[-\frac{A\dot{x}(t)}{\omega_0} + \frac{y(t)\dot{x}(t)}{\omega_D} - \frac{x(t)\dot{y}(t)}{\omega_0}\right]\left[-\frac{A\dot{x}(t+\tau)}{\omega_c} + \frac{y(t+\tau)\dot{x}(t+\tau)}{\omega_0} - \frac{x(t+\tau)\dot{y}(t+\tau)}{\omega_D}\right]\right\} \tag{5}$$

By rewriting Equation 5 as the sum of expected values and simplifying, the autocorrelation becomes

$$R_{zz}(\tau) = \frac{A^2}{\omega_0^2}\frac{d^2R_{xx}(\tau)}{d\tau^2} + \frac{2}{\omega_c^2}R_{yy}(\tau)R_{\dot{x}\dot{x}}(\tau) - \frac{2}{\omega_0^2}\left[\frac{dR_{xx}(\tau)}{d\tau}\right]^2 \tag{6}$$

The Fourier transform of $R_{zz}(\tau)$ will produce the output power spectral density (PSD), or,

$$R_{zz}(\tau) \Longleftrightarrow S_{zz}(f) \text{ WATTS/Hz} \tag{7}$$

$$S_{zz}(\omega) = \frac{A^2}{\omega_0^2}\left[\omega^2 S(\omega)\right] + \frac{2}{\omega_0^2}\left\{\mathcal{F}\left[R_{yy}(\tau)R_{\dot{x}\dot{x}}(\tau)\right]\right\} - \frac{2}{\omega_0^2}\mathcal{F}\left\{\left[\frac{dR_{xx}(\tau)}{d\tau}\right]^2\right\}, \tag{8}$$



328

where $S(\omega)$ is as shown in Figure 3a.

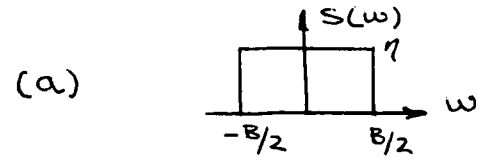


Figure 3a. PSD of x(t) and y(t)

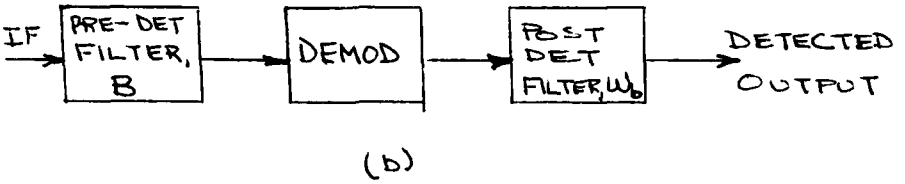


Figure 3b. Complete Detector

The second and third terms of Equation 8 may be evaluated using convolution techniques. After extensive manipulation, the output PSD becomes

$$S_{zz}(\omega) = \frac{A^2}{\omega_0^2}\left[\omega^2 S(\omega)\right] + \frac{1}{\pi\omega_0^2}\begin{bmatrix} \eta^2/3\left[(\omega+\frac{B}{2})^3+(\frac{B}{2})^3\right], & -B\le\omega<0 \\ \eta^2/3\left[(-\omega+\frac{B}{2})^3+(\frac{B}{2})^3\right], & 0\le\omega\le B \end{bmatrix} + \frac{1}{\pi\omega_0^2}\begin{bmatrix} \eta^2\left[\frac{2}{3}(\frac{B}{2})^3+(\frac{B}{2})^2\omega-\frac{\omega^3}{6}\right], & -B\le\omega\le-\frac{B}{2} \\ \eta^2\left[\frac{\omega^3}{2}-\frac{2(\frac{B}{2})^3}{3}-(\frac{B}{2})^2\omega\right], & -\frac{B}{2}\le\omega\le 0 \\ \text{(SYMMETRIC IN POSITIVE HALF PLANE)} \end{bmatrix}. \quad (9)$$

where B is the predetection bandwidth (Figure 3b).

The output noise power is determined by integrating Equation 9 over the post detection bandwidth (Equation 10).

$$\text{Noise Power} = \frac{1}{2\pi}\int_{-\omega_b}^{\omega_b} S_{zz}(\omega)\, d\omega \qquad (10)$$

where $\omega_b$ is the post detection bandwidth.

Completing the integration results in Equation 11.

$$\text{Noise Power} = \frac{A^2\eta\omega_b^3}{3\pi\omega_0^2} + \frac{\eta^2\omega_b^4}{24\pi^2\omega_0^2} + \frac{\eta^2\omega_b^3 B}{6\pi^2\omega_0^2} - \frac{\eta^2\omega_b^2 B^2}{4\pi^2\omega_0^2} + \frac{\eta^2\omega_b B^3}{6\pi^2\omega_0^2}. \qquad (11)$$

In order to obtain the output signal to noise ratio, the signal output power from the demodulator must also be obtained. Single tone modulation is a common standard of comparison. Assuming single tone modulation, the input signal can be written as

$$\text{Input Signal} = A\cos(\omega_0 t + \beta \sin\omega_M t), \qquad (12)$$

where $\beta$ = modulation index

and $\omega_M$ = frequency of modulating signal.

Passing this signal through the demodulator yields

$$\text{Output Signal Power (RMS)} = \frac{A^4 \beta^2 \omega_M^2}{2\omega_0^2} \qquad (13)$$

The SNR at the detector output is simply the ratio of Equations 11 and 13, or, (assuming signal and noise can be taken additively)

$$SNR = \frac{\frac{3}{2}(CNR) B \beta^2 \frac{\omega_M^2}{\omega_b^3}}{1 + \frac{\omega_b}{8B(CNR)} + \frac{1}{2(CNR)} - \frac{3B}{4\omega_b(CNR)} + \frac{B^2}{2\omega_b^2(CNR)}} \qquad (14)$$

This result is exceedingly simple. It is valid above threshold, at threshold, and below threshold. Only three assumptions were made in this derivation:

(1) $\omega_0^2 >> \omega_0$

(2) The signal and noise are additive.

(3) $\omega_b < \frac{B}{2}$

Special Case--High CNR

For the high CNR case the last four terms in the denominator of Equation 14 become negligible. Hence,

$$SNR(\text{For High CNR}) = \frac{3}{2}(CNR) B \beta^2 \frac{\omega_M^2}{\omega_b^3} \qquad (15)$$

Setting $\omega_M = \omega_b$ and recalling that

$$CNR_{AM} = CNR\ (B/2\omega_b),$$

Equation 15 may be reduced to

$$SNR\ (High\ CNR) = 3\beta^2 CNR_{AM}$$

Equation 17 describes the SNR improvement expected in the linear improvement region. This expression is identical to the well known expression for the conventional limiter discriminator above threshold.[2] Hence, the performance of the Klapper-Kratt detector above threshold is identical to that of the limiter discriminator above threshold, without the use of a limiter. A conventional discriminator, however, has a highly degraded performance without a limiter.

Threshold

Equation 14 may be used to determine threshold occurence for a specified $\omega_b$ and B. This equation has been evaluated for various values of the ratio $B/2\omega_b$ , and the result is plotted in Figure 4.

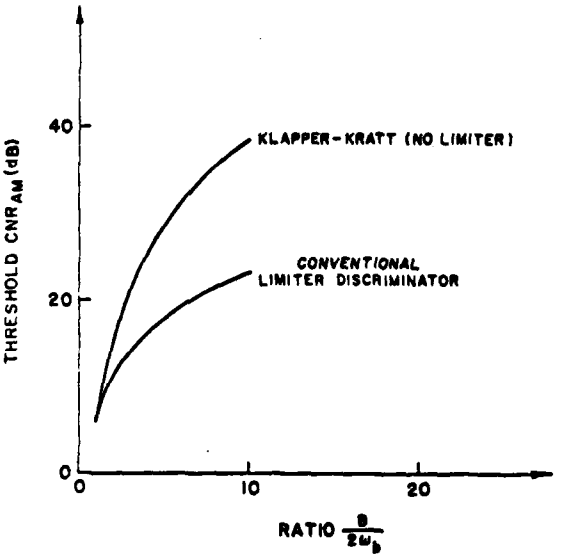


FIGURE 4 THRESHOLD $CNR_{AM}$ VS IF TO BASE BAND RATIO

Comparing this curve with that of the limiter discriminator shows no apparent threshold improvement as was previously thought. However, the new detector, without the additional complexity of a limiter, will

perform nearly as well as the limiter discriminator for low modulation indices.

## RF Cancelling

Up to this point of the analysis the RF cancelling portion of the detector has been ignored. It has been assumed that the canceller simply eliminates the undesired high frequency products of detection, and has no effect on the output signal to noise ratio. This assumption is, in fact, true as can be demonstrated by following the signal plus noise through the canceller. This derivation will not be included in this paper. It is straight-forward, but lengthy.

## Experimental Verification

The demodulator portion of the dual differentiator version of the Klapper-Kratt detector has been built and tested. Data taken with this demodulator is presented for comparison with the analytical results of the preceding paragraphs.

The circuitry, assembled with silicon monolithic integrated circuits, is shown in Figure 5.

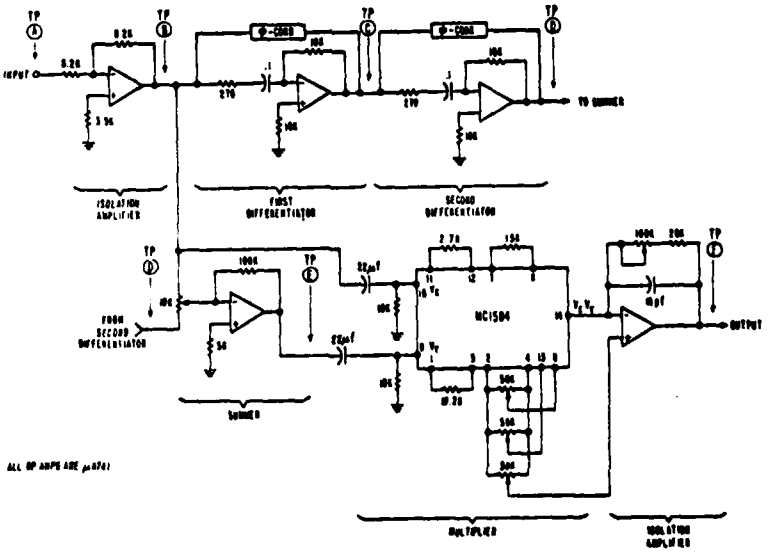


FIGURE 5 DEMODULATOR CIRCUIT DIAGRAM

A center frequency of 1000 Hz. was chosen for convenience. Adjustable, active, electronic filters were used to establish pre- and post-detection filtering. The predetection filter bandwidth was set to 165 Hz., while the post-detection filter was adjusted to a bandwidth of 32 Hs. A 25 Hz. baseband modulating signal was used to deviate the carrier $\pm$ 75 Hz. A plot of the measured SNR versus CNR characteristic for the Klapper-Kratt demodulator is shown in Figure 6.

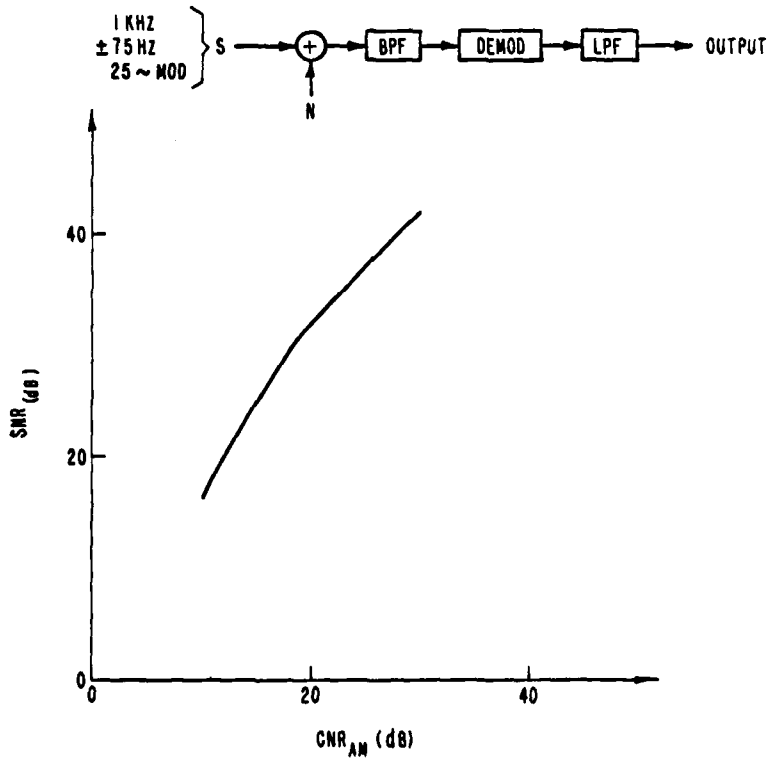


FIGURE 6. EXPERIMENTAL PERFORMANCE OF KLAPPER-KRATT DEMODULATOR WITHOUT LIMITER

Figure 7 is an expanded portion of Figure 6. Figure 7 shows threshold occurring at $CNR_{AM}$ = 16.9 dB; the SNR improvement above threshold is 12.3 dB. A conventional limiter discriminator was assembled and evaluated for comparison.

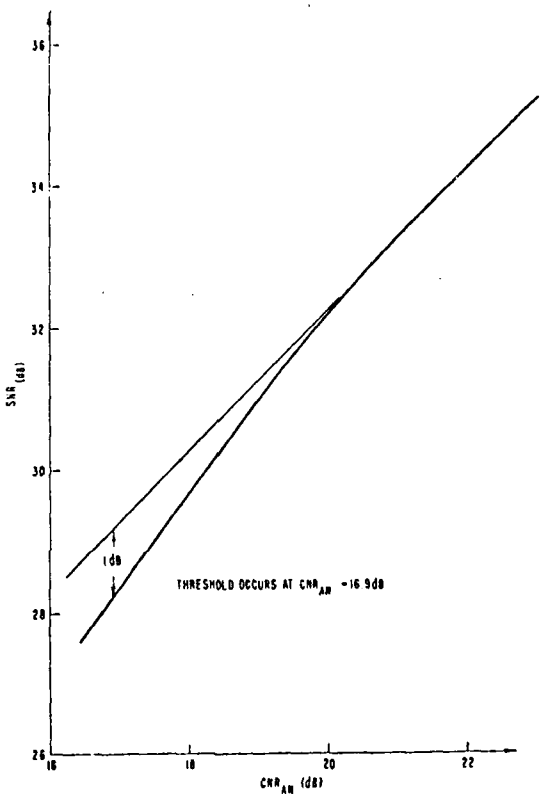


FIGURE 7 EXPERIMENTAL PERFORMANCE OF KLAPPER-KRATT DEMODULATOR WITHOUT LIMITER (EXPANDED SCALE)

Figure 8 and Table I present a comparison of the experimental and analytical data gathered in this investigation of the noise performance of the Klapper-Kratt detector. The graphical comparison shows excellent agreement above and below threshold. These curves, while not coincident, are quite similar in the vicinity of threshold. The small ( $\prec$ 1.0 dB) differences between the measured and analytical SNRs produce the 3.0 dB difference in the experimental versus analytical threshold CNRs. From Figure 8 it is clear that the Klapper-Kratt detector (no limiter) performs the same as the limiter discriminator above threshold. Threshold in the Klapper-Kratt detector, however, occurs at a higher CNR than that of the limiter discriminator. This result led to the experimental investigation of the Klapper-Kratt

detector with the addition of a limiter.

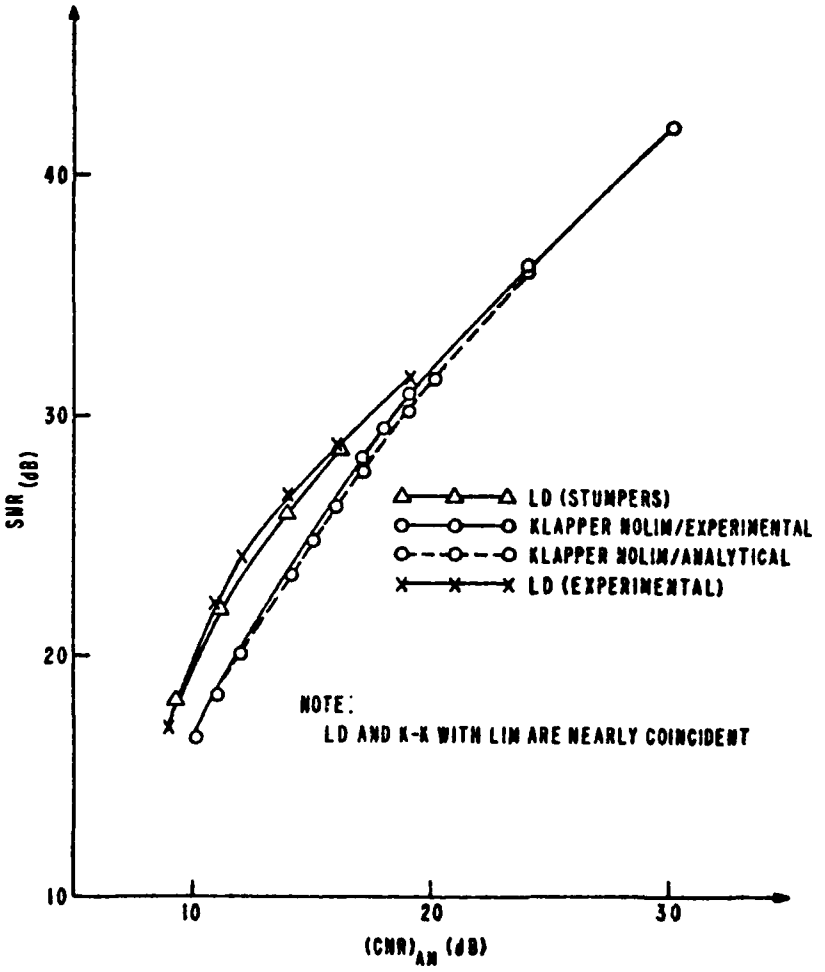


8.

FIGURE [redacted] ANALYTICAL AND EXPERIMENTAL COMPARISON OF THE KLAPPER-KRATT AND LIMITER DISCRIMINATOR DEMODULATORS

| $CNR_{AM}$ (dB) | | ANALYTICAL | | EXPERIMENTAL | |
|---|---|---|---|---|---|
| | | Improve. | Threshold | Improve. | Threshold |
| LIMITER DISCRIMINATOR | | 12.2 | 12.5 | 12.6 | 11.5 |
| KLAPPER KRATT | NO LIMITER | 12.2 | 19.9 | 12.3 | 16.9 |
| | WITH LIMITER | --- | --- | 12.6 | 11.2 |

TABLE I. COMPARISON OF THE LIMITER DISCRIMINATOR WITH THE KLAPPER-KRATT DEMODULATOR

Results of this investigation are shown in Figure 9.

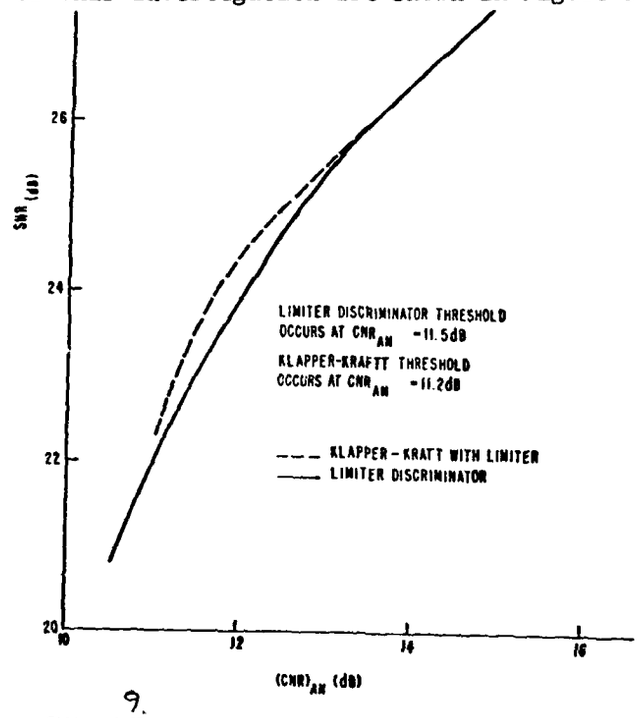


FIGURE 9. COMPARISON OF KLAPPER-KRATT DEMODULATOR (WITH LIMITER) AND LINITER DISCRIMINATOR

The performance of the Klapper-Kratt detector (with limiter) is virtually identical to that of the conventional limiter discriminator.

## Conclusions

In the above threshold region the Klapper-Kratt detector performs identically to the limiter discriminator. Threshold in the Klapper-Kratt detector occurs at a higher CNR than that of the limiter discriminator. For small or moderate modulation indices this difference in threshold performance is quite small. Small enough, in fact, that in applications where a limiter is undesirable the Klapper-Kratt detector would likely be a preferred alternative to the conventional limiter discriminator. The primary application for this demodulator is where delay must be minimized.

The equation describing the performance of the new demodulator is very simple. This result is valid in the linear improvement region, at threshold, and in a region below threshold.

TARBELL

REFERENCES:


1. J. Klapper & E. Kratt, "A New Family of Low Delay FM Detectors" , IEEE Transactions on Communications, February, 1979.

2. J. Klapper & J. Frankle, Phase-Locked and Frequency-Feedback Systems, Ch. 3, Academic Press, 1972.

3. L. Stumpers, "Theory of Frequency Modulation Noise" , Proc. IRE, Vol 36, No 9, p.1081-92, September, 1948.




339 - 340x


DATE
ILME